

4. S. Nikonov *et al.*, *Grudn. Serdech. Sosudist. Khir.* **2**, 42 (1991).
5. E. Cozzi and D. J. White, *Nature Med.* **1**, 964 (1995).
6. D. White, *Nature* **378**, 434 (1995).
7. *Animal to Human Transplants: The Ethics of Xenotransplantation* (Nuffield Council on Bioethics, London, 1996).
8. R. E. Benveniste and G. J. Todaro, *Proc. Natl. Acad. Sci. U.S.A.* **72**, 4090 (1975).
9. M. M. Lieber *et al.*, *Virology* **66**, 616 (1975).
10. Q-One Biotech Ltd. and Imutran Ltd., patent application WO 97/40167 (1997).
11. C. Patience, Y. Takeuchi, R. A. Weiss, *Nature Med.* **3**, 282 (1997).
12. P. Le Tissier *et al.*, *Nature* **389**, 681 (1997).
13. D. E. Akiyoshi *et al.*, *J. Virol.* **72**, 4503 (1998).
14. U. Martin *et al.*, *Lancet* **352**, 692 (1998).
15. C. A. Wilson *et al.*, *J. Virol.* **72**, 3082 (1998).
16. Y. Takeuchi *et al.*, *ibid.*, p. 9986.
17. C. Patience *et al.*, *Lancet* **352**, 699 (1998).
18. T. E. Starzl *et al.*, *Hepatology* **17**, 1127 (1993).
19. C. Mullon and Z. Pitkin, *Exp. Opin. Invest. Drugs* **8**, 229 (1999).
20. M. E. Breimer, *Xenotransplantation* **3**, 328 (1996).
21. E. A. Hoover *et al.*, *J. Am. Vet. Med. Assoc.* **199**, 1392 (1991).
22. At GTI, DNA was isolated from PBMCs using a genomic DNA isolation procedure (QIAamp Blood Kit, Qiagen).
23. DNA (3.3 μ g) was amplified by PCR with primers 5'-AGCTCCGGGAGGCCTACTC-3' and 5'-ACAGC-CGTTGGGTGGTCA-3', probe 5'-FAM-CCACCGTG-CAGGAAACCTCGAGACT-TAMRA-3' [where FAM (6-carboxyfluorescein) is a fluorescent tag and TAMRA (6-carboxytetramethylrhodamine) is a fluorescence quencher], and the 7700 sequence detector system (ABI/Perkin-Elmer). The PCR was performed in a 100- μ l reaction volume containing 5 U of Taq polymerase and 1 U of UNG, 300 nM each primer, and 100 nM probe in the Universal Master Mix buffer (Perkin-Elmer). The cycling parameters were 2 min at 50°C, 10 min at 95°C, and 60 cycles of 15 s at 95°C and 1.5 min at 60°C.
24. A total of 10, 10², 10³, 10⁴, 10⁵, and 10⁶ copies of the *pol/env* plasmid in a background of 3.3 μ g of DNA from three species were used to prepare standard PERV *pol* curves. The validation consisted of three runs for each species, each of which included five PERV *pol* standard curves, five reagent controls, 45 negative controls, and 10 one-copy positive controls. Validation showed that the assay could detect one copy of PERV in a background of 500,000 human cells and that it was quantitative over a range of 10 to 10⁶ copies of PERV.
25. W. M. Switzer *et al.*, *Transplantation* **68**, 183 (1999).
26. DNA (0.66 μ g) was amplified using primers for the conserved region of the *pol* gene. Primers used were 5'-GCTACAACCATTAGGAAACTAAAAG-3' and 5'-AACCAGGACTGTATCTTGATCAG-3'.
27. DNA (3.3 μ g) was amplified by quantitative PCR with primers 5'-TAGCCATGCTGCATGTAATGC-3' and 5'-GGAGCGTGGCCCAAT-3', probe 5'-FAM-ATGCTG-CATGGAATGCACTACCTCAA-TAMRA-3', and the 7700 sequence detector system (ABI/Perkin-Elmer). The PCR was performed in a 100- μ l reaction volume containing 5 U of Taq polymerase and 1 U of UNG, 300 nM each primer, and 100 nM probe in 1 \times Universal Master Mix (Perkin-Elmer). The cycling parameters were 2 min at 50°C, 10 min at 95°C, and 40 cycles of 15 s at 95°C and 1.5 min at 60°C.
28. RNA was reverse-transcribed with a primer containing a 19-base sequence at the 3'-end specific for PERV *pol* and a 30-base tag sequence at the 5'-end, 5'-GAACATCGATGACAAGCTTAGTATCGATAACAG-CCGTTGGTGGTCA-3', for 30 min at 42°C using 50 U of MuLV reverse transcriptase (RT) followed by 10 min at 90°C. Control reactions with no RT were also performed as a control for contamination with PERV genomic DNA. After reverse transcription, the cDNA was amplified with primers specific for PERV *pol* (5'-AGTCCGGGAGGCCTACTC-3') and the cDNA specific 30-base tag primer (5'-GAACATCGATGACAAGCTTAGTATCGATA-3') and probe 5'-FAM-CCACCGTGAGGAAACCTCGAGACT-TAMRA-3'. Amplification was detected with the 7700 sequence detection system (ABI/Perkin-Elmer). The cycling parameters were 2 min at 50°C, 10 min at 95°C, and 42 cycles of 15 s at 95°C and 2 min at 65°C.
29. At Q-One, RNA was reverse-transcribed for 50 min at 42°C by means of 5 U of Moloney murine leukemia virus (MuLV) reverse transcriptase (RT) with random hexanucleotides. After transcription, ribonuclease H was added to the reaction mix, which was then heated to 37°C for 15 min. Control reactions with no RT were also performed as a control for contamination with PERV genomic DNA. After reverse transcription, 5 μ l of the sample was amplified using primers from within the PERV *gag* gene, 5'-GCGACCCAGC-CAGTTGCATA-3' and 5'-CAGTTCCTTGCCAGTG-TCCTT-3'. A second nested PCR assay was carried out using the primers 5'-TGATCTAGTGAGAGAG-GCAGAG-3' and 5'-CGCACACTGGTCTTGTCG-3'. RT-PCR products were analyzed by agarose gel electrophoresis.
30. Purified recombinant PERV protein or virions were treated with SDS/ β -mercaptoethanol and separated by electrophoresis through a tris-glycine acrylamide gel (12%) before immunoelectrotransfer onto PVDF membrane (Imobilon) (200 mA, 1 to 2 hours). The membrane was washed in phosphate-buffered saline (PBS)/Tween before being treated with milk protein. Test sera were diluted to 1:200 in PBS/Tween containing 5% milk protein and incubated with membranes for 1 to 2 hours at room temperature. Blots were washed in PBS/Tween and incubated with the secondary antibody, an alkaline phosphatase-labeled antiserum diluted at 1:1000, for 1 hour at room temperature. After incubation, the membrane was washed repeatedly in PBS/Tween and developed with 5-bromo-4-chloro-2-indolyl phosphate/nitro blue tetrazolium, which gives a dark blue precipitate when labeled antibody has bound. Negative controls were performed by incubating membranes with serum from individuals who had not been exposed to porcine tissues. The protein immunoblot assay was validated with serum samples from a variety of sources (200 healthy humans, 58 HIV-1-positive humans, 18 HIV-2-positive humans, 13 HTLV-positive humans, four butchers with lymphoma, 20 transplant patients, and 10 CMV-positive humans with transplants).
31. A. L. Matthews *et al.*, *Transplantation* **67**, 939 (1999).
32. R. F. Grant *et al.*, *Virology* **207**, 292 (1995).
33. Z. Long *et al.*, *Hum. Gene Ther.* **9**, 1165 (1998).
34. R. J. Biggar *et al.*, *Lancet* **ii**, 520 (1985).
35. J. Stoye, *ibid.* **352**, 666 (1998).
36. D. Onions, D. Hart, C. Mahoney, D. Galbraith, K. Smith, *Trends Microbiol.* **6**, 430 (1998).

1 June 1999; accepted 12 July 1999

Superconductivity and the *c* Axis Spectral Weight of High- T_c Superconductors

L. B. Ioffe and A. J. Millis

The temperature dependence of the *c* axis spectral weight (frequency integral of the interplane conductivity) of high transition temperature (high- T_c) superconductors is shown to be a probe of thermal and quantal fluctuations of the phase of the superconducting order parameter. The behavior of underdoped cuprates is shown to be a natural consequence of superconducting pairing without long-ranged phase coherence. Very underdoped cuprates are found to have strong phase fluctuations, even for temperatures much less than the transition temperature.

The frequency (ω) and temperature (T) dependence of the interplane conductivity σ_c is one of the long-standing mysteries of high-temperature superconductivity. Particular attention has focused on the spectral weight, the integral of the real part of the

conductivity over some frequency range, which has been observed (1-6) to have a strong temperature dependence in many high- T_c materials. This dependence on T was argued by some to be highly anomalous and to provide strong evidence in favor

of the "interlayer tunneling" model of high-temperature superconductivity (7-10). Other workers (11-14) have argued that some aspects of *c* axis transport can be understood in relatively conventional terms, but have not considered the temperature dependence of the spectral weight. Here, we present a theory of the *c* axis spectral weight, $K_c(T)$, which accounts for the data.

The high-temperature copper-oxide superconductors have a layered crystal structure in which the important structural subunit is the copper-oxide (CuO_2) plane, with interplane (that is, *c* axis) couplings much weaker than in-plane ones. The conductivity in the direction perpendicular to the planes, $\sigma_c(\omega, T)$, is a complex function with real ($\sigma_c^{(1)}$) and imaginary ($\sigma_c^{(2)}$) parts. We denote the spectral weight at frequencies less than Ω by $K(\Omega, T)$;

Department of Physics and Astronomy, Rutgers University, Piscataway, NJ 08854, USA.

E-mail: ioffe@physics.rutgers.edu (L.B.I.) and millis@physics.rutgers.edu (A.J.M.)

in the particular case of the c axis, the convenient definition is

$$K_c(\Omega, T) = \frac{a^2}{de^2} \int_0^\Omega \frac{2d\omega}{\pi} \sigma_c^{(1)}(\omega, T) \quad (1)$$

Here, a and d are in-plane and c axis lattice parameters, respectively, and e is the electric charge. Standard sum rule arguments (15) imply $K_c(\infty, T) = na^2/(dm)$, where n is the total density of carriers in the solid (including all conduction and valence bands and normalized per CuO_2 plane) and m is the electron mass. $K_c(\Omega < \infty, T)$ may have temperature dependence. This is, however, usually believed to be weak if Ω is chosen in a reasonable manner (that is, smaller than a typical interband transition frequency but larger than important low-energy scales such as $k_B T$ or the superconducting gap). In a superconductor, for example, the real part of the conductivity may be written (16)

$$\sigma^{(1)}(\omega, T) = \pi \rho_s(T) \delta(\omega) + \sigma^{\text{reg}}(\omega, T) \quad (2)$$

Here, $\sigma^{\text{reg}}(\omega, T)$ is a regular function of frequency coming from quasi-particle excitations, and the term proportional to $\delta(\omega)$ expresses the infinite dc conductivity of superconductor. The coefficient ρ_s of $\delta(\omega)$ defines the superfluid stiffness or strength of the superconducting order. As T is increased through the superconducting transition temperature T_c , $\rho_s \rightarrow 0$. In conventional superconductors, the superconducting gap Δ also vanishes at T_c , so that $\sigma^{\text{reg}}(\omega)$ increases for $\omega \sim 2\Delta$. Calculations confirm that the two effects cancel, so that $K(\Omega, T)$ has only a very weak T dependence for $\Omega \gg 2\Delta$ (16).

Weak T dependence of K has been ex-

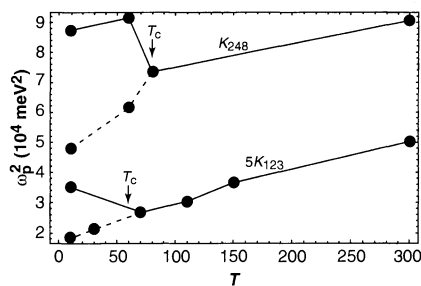


Fig. 1. Optical weight, $\omega_p^2 = \frac{4\pi de^2}{a^2} K_c(T)$, expressed as square of plasma frequency for $\text{YBa}_2\text{Cu}_4\text{O}_8$ and $\text{YBa}_2\text{Cu}_3\text{O}_{6.6}$. Below T_c , we show both the full weight (solid line) and the weight from σ^{reg} (dashed line). For $\text{YBa}_2\text{Cu}_4\text{O}_8$, the contributions to $K_c(T)$ from σ^{reg} were obtained by integrating the curves presented in figure 2 of (7) over the available range of frequencies ($\Omega \approx 700 \text{ cm}^{-1}$), while the superfluid contribution is presented in figure 3 of the same work. For $\text{YBa}_2\text{Cu}_3\text{O}_{6.6}$, the contribution from σ^{reg} (also integrated up to $\Omega \approx 700 \text{ cm}^{-1}$) is presented in figure 11 of (3), and the superfluid part is given in (6).

perimentally verified in many cases, including the in-plane conductivity of high-temperature superconductors (17), but is conspicuously violated by the c axis conductivity of high- T_c materials (1-6). The manner in which the sum rule is violated depends on the doping state: optimal doping (the doping level which maximizes T_c), overdoping, and underdoping. We focus here on underdoped materials, which display the most anomalous properties.

In underdoped cuprates, the room-temperature conductivity is very small, and is roughly constant over a wide frequency range. As T is decreased, a normal state "pseudogap" opens at a temperature $T_{\text{PG}} \approx 200$ to 300 K , much greater than T_c . The pseudogap is characterized by a frequency scale $2\Delta^* \sim 40 \text{ meV}$ and is also observed in nuclear magnetic resonance (18, 19), tunneling (20, 21), photoemission (22, 23), and in-plane optical conductivity (8, 17). For frequencies $\omega < 2\Delta^*$, $\sigma_c^{(1)}$ decreases as T is decreased below T_{PG} , but no compensating increase is observed at higher frequencies (at least in the range $\omega < 0.5 \text{ eV}$, where the physics is clearly due to conduction-band excitations). Thus, $K_c(0.5 \text{ eV}, T)$ decreases as T is decreased below T_{PG} (3, 5, 6). By contrast, for the in-plane conductivity, a decrease in the frequency range $\omega \sim 2\Delta^*$ is compensated by an increase at lower frequencies, leading to a very weak T dependence of the in-plane $K(T)$ (8, 17).

As T is further decreased below T_c , $\sigma_c(\omega \leq 2\Delta^*)$ continues to decrease and a superfluid contribution appears at $\omega = 0$. As noted by many authors (3, 5, 6, 9), in underdoped materials, the increase in ρ_s is greater than the weight lost from σ^{reg} so that the spectral weight increases below T_c . The T dependence of the spectral weight is shown in Fig. 1 for the prototypical underdoped materials $\text{YBa}_2\text{Cu}_3\text{O}_{6.6}$ (3) and $\text{YBa}_2\text{Cu}_4\text{O}_8$ (1). In both systems, there is a decrease in K_c as T is decreased from room temperature to T_c followed by an increase as T is decreased from T_c to the lowest measured temperature. In $\text{YBa}_2\text{Cu}_4\text{O}_8$, the increase as $T \rightarrow 0$ restores the weight lost as T is decreased from room temperature to T_c , whereas in $\text{YBa}_2\text{Cu}_3\text{O}_{6.6}$ it does not. In both materials, the increase below T_c is about twice the weight lost from σ^{reg} between $T = T_c$ and $T = 0$. A recent paper (6) argues that this factor of two occurs in all underdoped materials, but other data suggest that it may not occur in the $\text{La}_{2-x}\text{Sr}_x\text{CuO}_4$ system at any doping (4). The increase of spectral weight below T_c has been a main focus of theoretical attention, especially in the context of the interlayer tunneling model (9, 10).

We now turn to the theory. We assume that high- T_c materials may be described by a Hamiltonian involving a single band of electrons moving in CuO_2 planes and subject to a weak between-planes hopping

$$H = H_{\text{in-plane}}$$

$$+ \sum_{p,\alpha,i} t_{\perp}(p) (c_{p,\alpha,i}^{\dagger} c_{p,\alpha,i+1} + c_{p,\alpha,i+1}^{\dagger} c_{p,\alpha,i}) \quad (3)$$

Here $c_{p,\alpha,i}^{\dagger}$ creates an electron of in-plane momentum p and spin α in plane i of the crystal, $H_{\text{in-plane}}$ is the Hamiltonian describing motion in a single CuO_2 plane (whose precise form we will not need to specify), and $t_{\perp}(p)$ is the hopping matrix element describing interplane motion of conduction electrons with in-plane momentum p . The crystal chemistry of high- T_c materials implies $t_{\perp}(p) \sim [\cos(p_x) - \cos(p_y)]^2$ (24) so that the interplane coupling is dominated by states near the $(\pi, 0)$ and $(0, \pi)$ points of the Brillouin zone, which are van Hove points of the two-dimensional band structure and are the points at which the superconducting gap is maximal. States near the zone diagonals, which are also the locations of the nodes of the superconducting gap, make a negligible contribution to interplane transport (25). As written, H describes "single-plane" cuprates such as $\text{La}_{2-x}\text{Sr}_x\text{CuO}_4$ or $\text{Tl}_2\text{CaCuO}_6$; various modifications which we will not explicitly mention are needed to describe bilayer materials such as $\text{YBa}_2\text{Cu}_3\text{O}_{6+x}$. The most important is that, especially in optimally-doped $\text{YBa}_2\text{Cu}_3\text{O}_7$ and in $\text{YBa}_2\text{Cu}_4\text{O}_8$, the CuO_2 chains break the tetragonal symmetry so that $t_{\perp}(p)$ does not vanish along the zone diagonal. This has consequences for the detailed frequency- and temperature-dependence of the conductivity, but is less important for the spectral weights we study here.

The layered crystal structure implies that t_{\perp} is much less than any important in-plane energy scale $E_{\text{in-plane}}$; we will therefore expand to the second order in the parameter $t_{\perp}/E_{\text{in-plane}}$. At this order, the interplane conductivity may be computed from the normal and anomalous in-plane Green functions $G(p, \omega_n) = \int d\tau e^{i\omega_n \tau} \langle T_{\tau} c_p(\tau) c_p^{\dagger}(0) \rangle$ and $F(p, \omega_n) = \int d\tau e^{i\omega_n \tau} \langle T_{\tau} c_p(\tau) c_p(0) \rangle$ which are defined and discussed in standard texts, for example in (26). To derive the expression, one represents the applied c axis electric field by a vector potential $\vec{A} = cE/i\omega$ coupled to H via the usual Peierls phase factor

$t_{\perp}(p) c_{p,\alpha,i}^{\dagger} c_{p,\alpha,i+1} \rightarrow t_{\perp}(p) c_{p,\alpha,i}^{\dagger} c_{p,\alpha,i+1} e^{i\vec{c} \cdot \vec{A} d}$ and calculates to second order in t_{\perp} and \vec{A} . The result, in Matsubara formalism, is

$$\sigma_c(\Omega, T) = \frac{e^2 d}{a^2} \frac{K_c(T) + \chi(\Omega, T)}{i\Omega} \quad (4)$$

with

$$K_c(T) = 2T \sum_{n,p,\sigma} t_{\perp}^2(p) [-G_{i,p}(\omega_n) G_{i+1,p}(\omega_n) + \langle F_{i,p}^+(\omega_n) F_{i+1,p}(\omega_n) \rangle + H.c.] \quad (5)$$

and

$$\chi(\Omega, T) = 2T \sum_{n,p,\sigma} t_{\perp}^2(p) [G_{i,p}(\omega_n^+) G_{i+1,p}(\omega_n) + \langle F_{i,p}^+(\omega_n^+) F_{i+1,p}(\omega_n) \rangle + H.c.] \quad (6)$$

where $\omega_n^+ = \omega_n + \Omega$. Note that we have written the term involving the F functions as an expectation value, because it depends on the phase coherence between planes. The superfluid stiffness in the c direction is given by (26)

$$\rho_s(T) = K_c(T) + \chi(0, T) = 4T \sum_{n,p,\sigma} t_{\perp}^2(p) \langle F_{i,p}^+(p, \omega_n) F_{i+1,p}(p, \omega_n) + H.c. \rangle \quad (7)$$

The total c axis oscillator strength contained in optical transitions described by H in Eq. 3 is given by K_c , as may be seen (27) by taking the $\Omega \rightarrow \infty$ limit of the Kramers-Kronig relation $\sigma^{(2)}(\Omega) = \int \frac{dx}{\pi} \sigma^{(1)}(x)/(\Omega-x)$ and noting that $\lim_{\Omega \rightarrow \infty} \chi \sim 1/\Omega$. The total c axis oscillator strength of the real material has contributions from transitions involving bands not included in Eq. 3 and is therefore greater. Manipulations show that K_c is the change in the total energy $E = \langle H \rangle$ due to switching on $t_{\perp}(p)$, that is

$$K_c = \int \frac{d^2p}{(2\pi)^2} t_{\perp}(p) \frac{\partial E}{\partial t_{\perp}(p)} \quad (8)$$

This equation can be also represented as $K_c \sim \sum_{p,\alpha,i} t_{\perp}(p) \langle c_{p,\alpha,i}^{\dagger} c_{p,\alpha,i+1} \rangle$; the expectation value is commonly referred to as c axis kinetic energy (6, 9). We believe that Eq. 8 provides more physical insight because in weakly coupled materials, contribution to the energy which depends on $t_{\perp}(p)$ comes from the vicinity of the Fermi surface, and these states are strongly affected by the changes introduced by superconductivity.

For example, for noninteracting electrons, one finds from Eq. 8 that for $T > t_{\perp}(p)$, $K_{c, \text{non-int}}(T) = -4 \int d^2p / (2\pi)^2 |t_{\perp}(p)|^2 \partial f / \partial \epsilon_p$ where f is the Fermi function, so $K_{c, \text{non-int}}$ is determined by states within an energy T of the Fermi surface. We contrast this with the result (valid for noninteracting and interacting electrons) (27, 28) for the conduction-band in-plane spectral weight $K_{\text{in-plane}}(T) = \langle -\sum_{p,\sigma} \partial^2 \epsilon_p / \partial p^2 c_{p,\sigma}^{\dagger} c_{p,\sigma} \rangle$ which is determined by a sum over all occupied momentum states in the band. Most of these are far from the Fermi level and therefore have occupations which depend only very weakly on temperature, so $K_{\text{in-plane}}$ depends only weakly on temperature [typically $O(T^2/E_{\text{in-plane}})$].

The difference between the in-plane and c axis spectral weights may be understood physically. Consider two coupled planes: for noninteracting electrons at $t_{\perp} = 0$, the eigenstates are a twofold degenerate set of Bloch states with in-plane dispersion ϵ_p . Application of the perturbation $t_{\perp}(p)$ splits the bands into two, with

energies $\epsilon_p \pm t_{\perp}(p)$; but except for p very near p_F , both states are either occupied or unoccupied, so that the total energy of these states does not change. However, for states very near the Fermi level, one band is occupied and one is empty, and a dependence on t_{\perp} results. These considerations are qualitative, but demonstrate the important point that changes in Fermi surface properties or in other aspects of the low-energy physics may change the c axis spectral weight substantially, even though the in-plane spectral weight is not significantly modified.

We turn now to the effects of superconductivity on the oscillator strength. The superconducting order parameter has an amplitude and a phase. A nonzero amplitude tends to open a gap in the electron spectrum, while long-ranged phase coherence leads to infinite conductivity and flux exclusion. Quantal and thermal effects cause the phase to fluctuate around its average value. It is even possible to have a nonzero amplitude without long-ranged phase coherence, and several authors have argued that precisely this phenomenon occurs in the pseudogap regime of underdoped high- T_c materials (29-31). Equations 5 and 7 make an interesting prediction for this case. At $T = 0$, the total spectral weight is given by Eq. 5. At $T \geq T_c$, $\langle F^+ F \rangle = 0$, so that $K_c(T \geq T_c) = -4T \sum_n \int d^2p / (2\pi)^2 t_{\perp}(p)^2 G(p, \omega_n)^2$. If the gap [at least in the $(0, \pi)$ region important for c axis conductivity] does not significantly change between $T = 0$ and $T = T_c$ and is sufficiently larger than T_c , then the integral over the product of G -functions at $T \sim T_c$ is equal to its value at $T = 0$, and from Eq. 7 we find

$$\rho_s = 2[K(T \sim T_c) - K(T = 0)], \quad (9)$$

We emphasize the generality of this result: the only assumptions made are (i) weak interplane coupling and (ii) the gap (at the momenta relevant for σ_c) is large compared with T_c and has negligible temperature dependence between $T = 0$ and $T = T_c$ (that is, $\int GG$ has negligible T dependence between T_c and $T = 0$). These assumptions are fulfilled in many underdoped high- T_c materials, and just this factor of two was recently reported in figure 3 of (6). As the doping level is increased toward optimal, the gap at $T \approx T_c$ decreases relative to T_c [$\Delta(T_c)/T_c \rightarrow 0$], and the situation becomes better described by the conventional theory in which $\rho_s = [K(T \sim T_c) - K(T = 0)]$.

The result (9) depends crucially on the assumption (29, 30) that the pseudogap is caused by pairing without long-ranged phase coherence. The agreement between our results and experimental data provides strong support for this hypothesis. Alternative models for the pseudogap (for example, short-ranged spin or charge density wave order) would yield a c axis spectral weight which does not depend on interplane phase coherence and would therefore not change significantly as T is increased from $T = 0$ to $T = T_c$. The generality of our argu-

ment, however, means that the factor of two observed in (6) provides no further insight into the microscopics of high- T_c materials. More insight is obtained from the ratio between the superfluid stiffness and the area lost below T_{PG} , which as we shall now show provides a measure of the strength of the quantal phase fluctuations in the superconducting state. In the absence of quantal fluctuations, the $T = 0$ product $\langle F_{i,p}^+(p, \omega_n) F_{i+1,p}(p, \omega_n) \rangle$ is equal to the same-plane correlator $F_{i,p}^+(p, \omega_n) F_{i,p}(p, \omega_n)$, and we expect that $K(T = 0)$ is essentially equal to $K_{\text{tot}} = K(T > T_{PG})$ up to corrections $O(\Delta/\epsilon_F)$. We have verified this by explicit calculations within the usual theory of superconductivity of a Fermi liquid. We schematically write this as

$$K_{\text{tot}} = 2\int -GG + \langle FF \rangle \quad (10)$$

In the actual material, thermal and quantum fluctuations in each plane reduce the interplane FF correlator by a Debye-Waller factor α , defined by $\sum_{p,n} \langle F_i F_{i+1} \rangle = \alpha \sum_{p,n} F_i F_i$, so that we have

$$K_{\text{phys}} = 2\int -GG + \alpha FF \quad (11)$$

and

$$\rho_s = 4\int \alpha FF \quad (12)$$

In particular, at $T > T_c$, $\alpha = 0$ but if $T < T_{PG}$, the gap still reduces the G - G contribution to K_c , leading to a loss of spectral weight as observed.

Now define

$$K_{\text{missing}} = \frac{a^2}{de^2} \int_{0+}^{\infty} \frac{2d\omega}{\pi} [\sigma(\omega, T > T_{PG}) - \sigma^{\text{reg}}(\omega, T = 0)] \quad (13)$$

From this definition and Eqs. 10, 11, and 12, one finds that as $T \rightarrow 0$

$$\alpha(T = 0) = \frac{\rho_s(T = 0)}{\rho_s(T = 0) - K_{\text{missing}}} \quad (14)$$

so the quantum Debye-Waller factor α may be deduced from the ratio of $\rho_s(T = 0)$ to the weight lost below T_{PG} . We note that in the strongly correlated anisotropic situation considered here, fluctuations have a different effect than might be expected. Instead of broadening the superconducting δ -function while preserving its area, they mainly transfer the weight to very high energies.

A related mechanism for reduction of $\rho_s(T = 0)$ was presented by Kim (32) who considered a model in which interplane transport occurred via an impurity scattering process which did not conserve momentum and thus, in a d -wave superconductor reduced the interplane FF correlator relative to the same-plane one. This mechanism would predict that even optimally doped materials and $\text{YBa}_2\text{Cu}_3\text{O}_8$ would have a $\rho_s(T = 0)$, which is smaller than the

missing area below T_c , in contrast with the data. The impurity model seems to us to be unphysical, but (32) is important because it draws attention to the interplane FF correlator and shows explicitly that the c axis sum rule is less robust than the in-plane one.

The general arguments we present are confirmed by calculations of $\sigma_c(\omega, T)$. The crucial ingredient in these calculations is the in-plane electron self energy which represents the non-trivial in-plane physics. We have investigated a variety of model self energies; the results will be published elsewhere.

To conclude, we review several qualitative features of the data in light of our results. In underdoped cuprates, the formation of the pseudogap does not lead to an increase in $\sigma_c(\omega)$ at any observed frequency. If the pseudogap were due to an incipient density wave instability, spectral weight lost below the gap would reappear as a peak in $\sigma_c(\omega)$ just above the gap, in contradiction with the data. On the other hand, we show that superconducting pairing without long-ranged order leads to the observed behavior. Our results therefore provide additional strong evidence that the pseudogap is caused by superconducting pairing and not by an incipient density wave. Second, the fact that the spectral weight restored at $T \rightarrow 0$ does not compensate all of the weight lost by gap formation in underdoped $\text{YBa}_2\text{Cu}_3\text{O}_{6.6}$, but yet compensates it in $\text{YBa}_2\text{Cu}_4\text{O}_8$, directly implies that in $\text{YBa}_2\text{Cu}_3\text{O}_{6.6}$, fluctuations reduce the value of the $T = 0$ interplane $F_i F_{i+1}$ correlator below the value of the same-plane correlator $F_i F_i$, while in $\text{YBa}_2\text{Cu}_4\text{O}_8$ they do not. There is other evidence (30) that $\text{YBa}_2\text{Cu}_3\text{O}_{6.6}$ has exceptionally large $T = 0$ fluctuations. A systematic comparison in a range of compounds of fluctuation strengths deduced from c axis conductivity and from other measurements would be interesting.

References and Notes

1. D. Basov, T. Timusk, B. Dabrowski, J. D. Jorgenson, *Phys. Rev. B* **50**, 3511 (1994).
2. S. L. Cooper and K. E. Gray in *Physical Properties of High-Temperature Superconductors IV*, D. M. Ginsberg, Ed. (World Scientific, Singapore, 1994), pp. 61–188.
3. C. C. Homes, T. Timusk, D. A. Bonn, R. Liang, W. N. Hardy, *Physica C* **254**, 265 (1995).
4. S. Uchida, K. Tamasaku, S. Tajima, *Phys. Rev. B* **53**, 14558 (1996).
5. S. Tajima *et al.*, *ibid.* **55**, 6051 (1997).
6. D. N. Basov *et al.*, *Science* **283**, 49 (1999).
7. P. W. Anderson, *ibid.* **268**, 1154 (1995).
8. A. V. Puchkov, D. N. Basov, T. Timusk, *J. Phys. Condens. Matter* **8**, 10049 (1996).
9. P. W. Anderson, *Science* **279**, 1196 (1998).
10. S. Chakravarty, *Eur. J. Phys. B* **5**, 337 (1998); S. Chakravarty, H.-Y. Kee, E. Abrahams, *Phys. Rev. Lett.* **82**, 2366 (1999).
11. R. J. Radtke and K. Levin, *Physica C* **250**, 282 (1995).
12. A. A. Abrikosov, *Phys. Rev. B* **54**, 12003 (1996).
13. N. Kumar, T. P. Pareek, A. M. Jayannavar, *ibid.* **57**, 13399 (1998).
14. S. Das Sarma and E. H. Hwang, *Phys. Rev. Lett.* **80**, 4752 (1998).
15. D. Pines and P. Nozières, *Theory of Quantum Liquids* (Addison-Wesley, Reading, MA, 1966).
16. M. Tinkham, *Introduction to Superconductivity* (McGraw-Hill, New York, 1996).
17. J. Orenstein *et al.*, *Phys. Rev. B* **42**, 6342 (1990).
18. M. Takigawa *et al.*, *ibid.* **43**, 243 (1991).
19. W. W. Warren Jr. *et al.*, *Phys. Rev. Lett.* **62**, 1193 (1989).
20. Ch. Renner, B. Revaz, J.-Y. Genoud, K. Kadowaki, O. Fischer, *ibid.* **80**, 149 (1998).
21. N. Miyakawa, P. Guptasarma, J. F. Zasadzinski, D. G. Hinks, K. E. Grey, *ibid.*, p. 157.
22. H. Ding *et al.*, *Nature* **382**, 51 (1996).
23. A. G. Loeser *et al.*, *Science* **273**, 325 (1996).
24. O. K. Andersen *et al.*, *J. Phys. Chem. Solids* **56**, 1573 (1995); O. K. Andersen *et al.*, *Phys. Rev. B* **50**, 4145 (1994).
25. L. B. Ioffe and A. J. Millis, *Phys. Rev. B* **58**, 11631 (1998).
26. J. R. Schrieffer, *Theory of Superconductivity* (Benjamin/Cummings, Reading, MA, 1983).
27. W. Kohn, *Phys. Rev.* **133**, A171 (1964).
28. A. J. Millis and S. N. Coppersmith, *Phys. Rev. B* **42**, 10807 (1990).
29. V. J. Emery and S. A. Kivelson, *Nature* **374**, 434 (1995).
30. V. B. Geshkenbein, L. B. Ioffe, A. I. Larkin, *Phys. Rev. B* **55**, 3173 (1997).
31. M. Franz and A. J. Millis, *ibid.* **58**, 14572 (1998).
32. E. H. Kim, *ibid.*, p. 2452.
33. We thank E. Abrahams for helpful discussions. A.J.M. thanks the NSF (grant DMR-9707701) for support.

12 April 1999; accepted 13 July 1999

Decreased Rates of Alluvial Sediment Storage in the Coon Creek Basin, Wisconsin, 1975–93

Stanley W. Trimble

The total measured rate of alluvial sediment accretion in the agricultural Coon Creek Basin for the period 1975–93 was only about 6 percent of the rate that occurred in the 1930s, but the distributed changes within the basin were highly variable and systematic. Sediment yield (efflux), however, remained relatively constant despite large stream and valley changes within the basin. These observations demonstrate (i) that sediment sources, sinks, and fluxes vary widely over time and space and (ii) that, although improved soil conservation measures have decreased soil erosion, the downstream effects are complex.

Erosion and sediment yield in any stream basin are rarely in a steady state. For monitoring environmental change, it is thus necessary to construct a sediment budget that accounts for storage fluxes within the basin during any time period (T). Here, I present results from a long-term study, attempting to account for the sediment budget over the 140-year period of European agriculture in Coon Creek, a typical agricultural basin of 360 km² in the Driftless Area of Wisconsin (Fig. 1). Measurements are largely based on surveyed and monumented stream and valley cross sections that have also received extensive stratigraphic studies for the agricultural period (2, 3). Over 150 such cross sections have been installed since 1938, of which 92 were recovered and resurveyed (see supplemental data, available at www.sciencemag.org/feature/data/1041853.shl). These resurveys were done from 1991 to 1995, but most were done in 1993; therefore, 1993 is used as the median date. Sediment yields were calculated by standard extrapolation techniques from measurements on the Grant River at Burton, Wisconsin, a similar basin ~90 km

south of Coon Creek (U.S. Geological Survey District Office, Madison, WI).

The major change in the sediment budget from earlier periods (Fig. 1) is the overall decrease in rates of storage, a trend that started in the 1940s and is directly attributed to improvements in agricultural land management (3, 4). From 1853 to 1938, an average of 405×10^3 Mg year⁻¹ of sediment went into storage (2, 3). This was reduced to 209×10^3 Mg year⁻¹ from 1938 to 1975 and then reduced to 80×10^3 Mg year⁻¹ from 1975 to 1993. These averages, however, disguise some striking shorter term rates. In the 1920s and 1930s (the period of maximum erosion and sediment storage), alluvial sediment accumulation in the basin was $\sim 1260 \times 10^3$ Mg year⁻¹ (3, 4). The recent (1975–93) rate of 80×10^3 Mg year⁻¹ is only ~6% of that highest rate. This decrease was due to improvements in land use and not due to a change in climate. Indeed, most of the period 1975–93 was wetter than average, with many large storms (5). A basin-wide 100-year flood occurred in 1978, and 1993 was also extremely wet.

Whereas sediment fluxes (sources and amounts) have changed drastically over the past 140 years, efflux, or sediment yield, has held relatively steady. This result demon-

Department of Geography and Institute of the Environment, University of California, 1255 Bunche Hall, Los Angeles, CA 90095–1524, USA.